Photoinitiated Synthesis and Characterization of P(MMA/DPB) Polymer Nanoparticles Using Poly(*N*-isopropylacrylamide) in Aqueous Solutions as a Template

Megh Raj Pokhrel, Katharine Janik, and Stefan H. Bossmann*

Lehrstuhl für Umweltmesstechnik, Engler-Bunte-Institut, Universität Karlsruhe, D-76128 Karlsruhe, Germany

Received September 21, 1999; Revised Manuscript Received February 14, 2000

ABSTRACT: The photoinitiated polymerization of methyl methacrylate (MMA) using 2,3-diphenylbutadiene (DPB) as cross-linking agent and benzoin (BN), benzoin methyl ether (BME), and irgacure (IGC) as photoinitiators in the presence of poly(*N*-isopropylacrylamide) (PNIPAM) as a water-soluble, hydrophobic template polymer in H_2O/DMF led to the formation of P(MMA/DPB) polymer latex particles. These particles were analyzed by using TEM in combination with the program IMAGE (NIH/USA). After purification by precipitation using THF/H_2O, globular latex particles were found. Using BME as photoinitiator, "real nanoparticles" possessing a smaller diameter than 10 nm were formed among bigger particles (d > 20 nm). The CHN analysis of the P(MMA/DPB) polymers indicated that a smaller fraction of PNIPAM (4−10%) was incorporated into the latex particles.

Introduction

Polymer latex particles formed by copolymerization of various monomers and cross-linking agents possess versatile physical properties,[1] and prior to our work, other tailored materials for applications especially in the biological and bioanalytical field have been proposed.[2] The size of the synthesized latex particles ranged in most cases from approximately 20 nm to several microns.[3] Only a few examples of real latex nanoparticles possessing diameters smaller than 10 nm are known to date.[4] Various methods for the preparation of latex particles have been reported in the literature. They rely on the formation of microdroplets of hydrophobic regions in an aqueous environment either before or during the polymerization process.[5] Anionic, cationic, and nonionic micelles, emulsions, microemulsions, and vesicles have been employed successfully.[6]

Compared to those bigger particles, nanoscopic polymer particles will have substantial advantages. Their reduced size will permit a faster response to environmental changes.[7] Furthermore, polymer nanoparticles will be used as building blocks for the nanoarchitecture of the future and for the tailoring of viable composite materials.[8] In this report we describe a method for the preparation of polymer nanoparticles using poly(*N*-isopropylacrylamide) in mixtures of water and the consonsolvent DMF as reaction template.

We have been inspired by Zhu and Napper, who investigated the stabilization of polystyrene latex particles in aqueous solutions by PNIPAM as well as the volume phase transitions of PNIPAM latex particles in H_2O/DMF mixtures.[9] PNIPAM is known to undergo a coil-to-globe transition of individual polymer chains in water (T = 32 °C) as well as many mixtures of water and water-mixable solvents.[10] The latter phenomenon was called co-nonsolvency, and ternary phase diagrams have been observed. On the basis of the solvent composition, characteristic LCST's (lower critical solution temperatures) were observed.[10] The investigation of spin-labeled PNIPAM in water and water/methanol applying CW-EPR indicated the extrusion of water as well as the preferential adsorption of methanol during the precipitation process, which is triggered by the increased hydrophobic interaction of individual polymer segments.[10] The analysis of the CW-EPR hyperfine coupling ($\langle A_N \rangle$) of the three-lined TEMPO spectrum indicated that PNIPAM forms strongly hydrophobic domains above the LCST temperatures in H_2O/MeOH, H_2O/THF, and H_2O/DMF. According to TEM results, the size of the individual nanodomains formed by the collapse of individual PNIPAM chains is in the range 2−20 nm.[11] The PNIPAM precipitate is then formed by the clustering of these individual PNIPAM nanostructures.[10] If conditions could be found where the size distribution of those PNIPAM nanodomains is very narrow, those *strongly hydrophobic domains* embedded by an aqueous environment would be a very promising reaction system. We attempted to test this hypothesis and are presenting first evidence of its capabilities to synthesize organic nanoparticles with a narrow size distribution. Other decisive factors with respect to (industrial) applications are the recovery of the template PNIPAM after reaction and the separation of the formed P(MMA/DPB) latex particles from the template.

PNIPAM, as polymerization template, methyl methacrylate (MMA), and 2,3-diphenylbutadiene (DPB) have been selected for the preparation of organic latex particles. MMA possesses a large chain propagation constant, and therefore, a good monomer consumption can be predicted. The reactivity of the cross-linking agent DPB toward the addition of radicals is also presumed to be high because of the resonance stabilization of the intermediary radical(s) formed. Polymerization was initiated photochemically because this method permits the independent selection of the reaction temperature during the formation of initial radicals. Benzoin (BN), benzoin methyl ether (BME), and irgacure (IGC) were selected as photoinitiators. Benzoin and its alkyl ether derivatives undergo the photochemical

* To whom correspondence should be addressed. E-mail: ie61@mv70.rz.uni-karlsruhe.de.

10.1021/ma991608z CCC: $19.00
Published on Web 04/27/2000

Scheme 1. Initial α-Cleavage of the Employed Photoinitiators after Absorption of a Photon in the Wavelength Region from 313 to 365 nm (According to Refs 12−14)

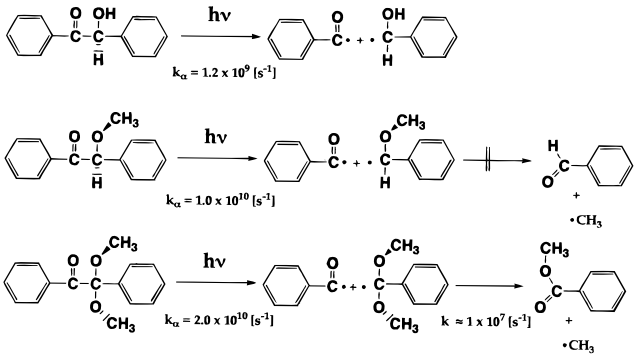

process named α-cleavage leading rapidly to benzoyl and substituted benzyl radicals ($k_\alpha > 10^{10}$ s^{-1}).[12] Therefore, it has been attributed either to an exceptionally rapid triplet process[12] or to a singlet reaction, which competes successfully with intersystem crossing.[13,14] Whereas the apparent quantum yield of IGC consumption in the wavelength region from 313 to 365 nm is close to unity,[15] the value of $\langle\Phi\rangle = 0.24$ for the disappearance of BME in benzene was determined.[13] No wavelength effect was observed! Furthermore, it has been concluded from polymerization experiments in comparison to BME that the apparent quantum yield for the α-cleavage of BN should be very similar to that of BME.[16] A value of $\langle\Phi\rangle = 0.19$ could be derived for BN. In Scheme 1 the photochemical reactions of the employed sensitizers are indicated.

Organic nano-latex particles adsorbed on a carbon surface were investigated by using TEM (transmission electron micrography).[17−20] Quantitative results are obtained when the TEM images are analyzed with the aid of a suitable computer software (IMAGE/NIH).[21] The size distribution was determined at a carbon surface, because the formed P(MMA/DPB) (nano)particles are not water-soluble. Other methods, such as quasi-elastic light scattering (QELS),[22] are therefore not applicable.

Experimental Section

Chemicals. DMF, AIBN, acetic acid, benzoin (BN), benzoin methyl ether (BME), irgacure (IGC), *N*-isopropylacrylamide (NIPAM), methyl methacrylate (MMA), 2,3-diphenylbutadiene (DPB), PMMA standards, 1,10-phenanthroline, and $(Fe)_2(SO_4)_3 \cdot 11H_2O$ were purchased from Fluka. THF, MeOH, *t*-BuOH, and *n*-hexane were received from Roth. Bidest. H_2O was used. Starburst dendrimers (SBD's) were purchased from the Michigan Molecular Institute.

General. The TEM images were recorded using a transmission electron micrograph EM 912/Zeiss equipped with an Omega filter system. In addition, a STI video camera was employed. For the analysis of the TEM images, the IMAGE software, generously provided by the National Institute of Health (NIH/USA), served as an excellent tool. Commercially available PAMAM starburst dendrimers (Aldrich) possessing distinct diameters and masses were deposited on identical carbon surfaces and used for the calibration of the IMAGE software. CHN analysis has been performed on a C, H, N, S analyzer (LECO Instruments). Details are indicated in the electronic supplementary index (ESI). A Haake VT5 viscometer was employed for standard measurements of PNIPAM solutions in THF. Poly(*N*-isopropylacrylamide) (PNIPAM) was prepared, purified, and analyzed according to standard procedures using AIBN in *t*-BuOH[23] ($[\eta] = 101 \pm 4$ [cm^3 g^{-1}]; $M\eta$ = 1 540 000 (calculated according to $\eta = 9.59 \times 10^{-3} M_v^{0.65}$); M_n = 77 400; M_w = 110 000; LCST = 32.1 °C). A polydispersity in the range of 1.4 was obtained, which is typical for thermal radical polymerization of acrylamides.[24]

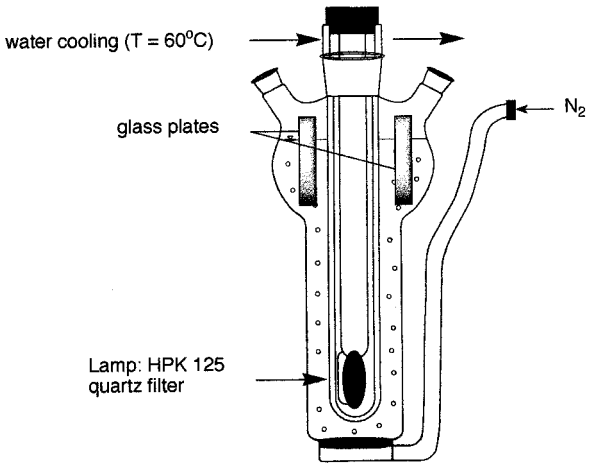

Figure 1. Photochemical bench reactor (V_{total} = 700 mL, $V_{(PNIPAM/H_2O/DMF)}$ = 500 mL) for photoinduced polymerization equipped with a water-cooled (T = 60 °C) mercury medium-pressure lamp (Philips HPK 125) and two glass scrubber plates (Pyrex: 2 × 10 cm^2 each). The reaction mixture was mediated vigorously by N_2 purging. The cooling trap for solvent recovery is not shown.

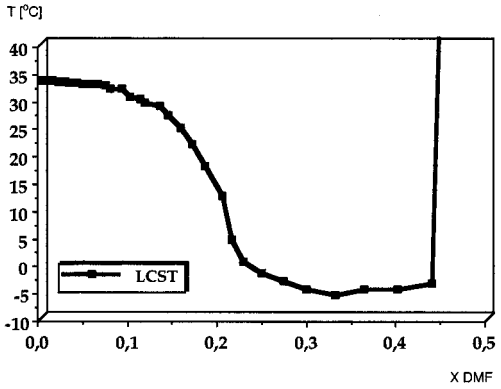

Figure 2. Ternary phase diagram of PNIPAM/H_2O/DMF (*X*: molar fraction of DMF).

Table 1. Apparent Quantum Yields $\langle\Phi\rangle$ and Apparent Reaction Rate Constants for the Photochemical Decomposition of Benzoin, Benzoin Methyl Ether, and Irgacure in 0.50 L of H_2O/DMF (70/30% per Weight) Containing 1.50 g of Precipitated PNIPAM (T = 60 °C)

initiator	$\langle\Phi\rangle^a$	k_{app} [s^{-1}]^b
BN	0.04 ± 0.01	(2.85 ± 0.18) × 10^{-4}
BME	0.26 ± 0.06	(3.53 ± 0.24) × 10^{-3}
IGC	0.37 ± 0.05	(4.75 ± 0.28) × 10^{-3}

[a] Apparent initial quantum yield for the photochemical decomposition of the photoinitiator by α-cleavage under polychromatic irradiation between 300 and 400 nm (HPK 125, main Hg lines: 313.1 and 366.6 nm). [b] Apparent reaction rate constants for the initiator consumption under continuous irradiation (HPK 125).

Photoinitiated Polymerization of Latex Particles. A 1.50 g sample of PNIPAM was dissolved in 0.50 L of H_2O/DMF (70/30% per weight) and warmed to 60 °C. The photochemical batch reactor employed in our experiments is schematically shown in Figure 1. As indicated in Figure 2, the LCST of PNIPAM is transcended at that H_2O/co-nonsolvent composition. The mixture was agitated and purged by a constant nitrogen flow for 30 min. Then 1.0 g of liquid MMA (1.0 × 10^{-2} mol), 0.10 g of solid DPB (4.845 × 10^{-4} mol), and 0.40 g of photoinitiator (BN, 1.885 × 10^{-3} mol; BME, 1.76 × 10^{-3} mol; IGC, 1.56 × 10^{-3} mol) were added. The N_2 purging continued

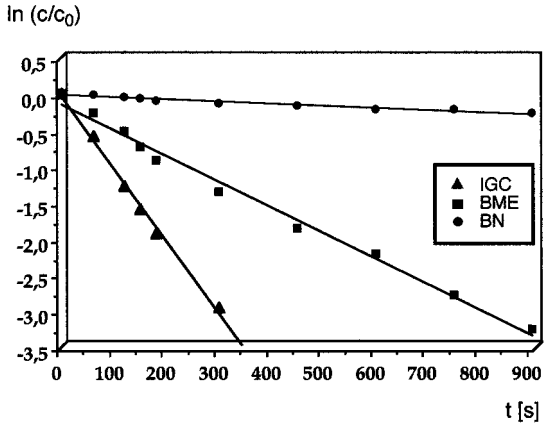

Figure 3. Consumption of the employed photoinitiators (initial concentrations: BN, 3.77×10^{-3} M; BME, 3.52×10^{-3} M; IGC, 3.12×10^{-3} M) under continuous irradiation by means of a HPK 125 mercury medium-pressure lamp.

for another 30 min. Then the reaction mixture was irradiated for 15 min at $T = 60$ °C. After photolysis the N_2 purging continued for an additional 15 min. During and after the photolysis, a pale yellow precipitate formed on the glass plates inside the reactor. (A little precipitation occurred at the quartz socket of the lamp as well.) Typical primary yields ranged from 0.48 to 0.38 g. The crude precipitate was reprecipitated by dissolving it in 10 mL of anhydrous THF followed by the addition of 1 mL of H_2O at $T = 20$ °C. The resulting white precipitate was then filtered off and dried in high vacuum. The following yields were obtained (BN/MMA/DPB, 0.26 ± 0.05 g (23%); BME/MMA/DPB, 0.28 ± 0.05 g (25%); IGC/MMA/DPB, 0.20 ± 0.05 g (18%)).

TEM Sample Preparation. The standard sample preparation procedure consisted of the dispersion of 0.50 mL of polymer latex particles dissolved in THF/H_2O (v/v: 1/1, $c = 1 \times 10^{-6}$ g L^{-1}) using a sonication system (Siemens). The microdroplets were deposited on a special TEM surface (available from Plano/Marburg) consisting of a copper net (distance of the copper wires: 85 μm), which are laminated with poly(vinylformaldehyde) (thickness: 20−40 nm). The PVF was sputtered using elementary carbon. This particular surface was exposed to the latex/solvent microdroplets for exactly 10 s (distance from the buffer surface: 5.0 cm). Finally, most of THF/H_2O water was removed in high vacuum over 24 h.

Gel Permeation Chromatography. The gel permeation chromatography (GPC) experiments were carried out employing an HP-79911 GP-103 column (PL Gel 10 μm, 1000 A, 7.5 × 300 mm). THF was used as eluent (0.50 mL min^{-1}). The concentration of the injected samples ($V_{inj} = 1.0$ μL) in THF was 1×10^{-3} g L^{-1}. Calibration of the GPC has been performed using five monodisperse PMMA samples (M_w = 2000, 8000, 30 000, 50 000, 75 000, 100 000, 150 000, and 200 000). The detection of the polymers was achieved using $\lambda = 220$ nm as detection wavelength.

HPLC Determination of the Photoinitiator Concentration. For quantitative HPLC analysis of BN, BME, and IGC an HP series II 1090 liquid chromatograph, equipped with a diode array detector (DAD) and a LiChrospher-100 RP 18 column and precolumn, was used (mobile phase: (0.10 mol L^{-1} $(C_2H_5)_3N/H_3PO_4$ (pH = 7.0)/acetonitrile, 65:35 v/v)). PNIPAM and P(MMA/DPB) latex particles were retained by the employed precolumn.

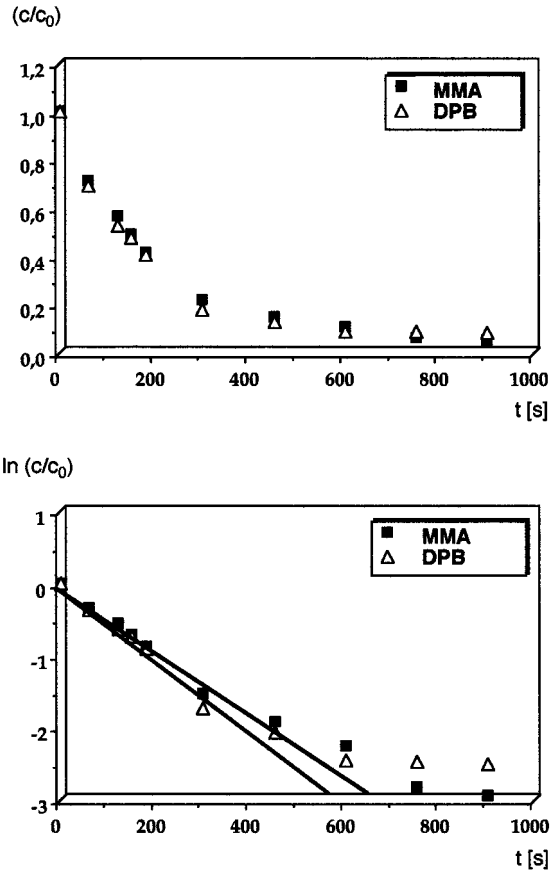

Figure 4. MMA and DPB conversion using BME as photoinitiator: 1.0 g of MMA (2.0×10^{-2} M), 0.10 g of DPB (9.69×10^{-4} M), and 0.40 g of BME (1.76×10^{-3} M) in 0.50 L of H_2O/DMF (70/30% per weight) under continuous irradiation between 300 and 400 nm.

Results and Discussion

Ferrioxalate Actinometry, Apparent Quantum Yields, and Reaction Rate Constants of Photoinitiator Consumption in PNIPAM/H_2O/DMF. The ferrioxalate actinometry procedures were described in detail in the literature.[25] The radiant power emitted by the employed medium-pressure mercury lamp (HPK 125, electrical power consumption 125 W; RP = 35.5 ± 1.3 W) was determined using ferrioxalate actinometry. Note that the precipitation of PNIPAM leads to an intense scattering effect.[26] For this reason and due to polychromatic irradiation, only apparent quantum yields and reaction rates could be obtained. The results are summarized in Table 1.

As seen in Table 1 and Figure 2, the initial quantum yield for the photochemical decomposition of BME

Table 2. Apparent Initial Quantum Yields for the Consumption of MMA and DPB and Apparent Reaction Rate Constants for MMA and DPB Consumption under Continuous Irradiation between 300 and 400 nm (HPK 125, Main Hg Lines: 313.1 and 366.6 nm)

initiator	$\Phi - [MMA]^a$	$-k_{app}$ [s^{-1}]^b	$\Phi - [DPB]^a$	$-k_{app}$ [s^{-1}]^b
BN	0.34 ± 0.02	$(8.08 \pm 0.04) \times 10^{-4}$	0.44 ± 0.035	$(1.05 \pm 0.06) \times 10^{-3}$
BME	1.43 ± 0.05	$(5.05 \pm 0.03) \times 10^{-3}$	1.59 ± 0.042	$(5.62 \pm 0.06) \times 10^{-3}$
IGC	3.06 ± 0.17	$(1.21 \pm 0.02) \times 10^{-2}$	3.56 ± 0.061	$(1.41 \pm 0.04) \times 10^{-2}$

[a] Apparent initial quantum yield for the consumption of MMA (or DPB) calculated according to the corresponding light absorption of the employed photoinitiator under polychromatic irradiation between 300 and 400 nm (HPK 125, main Hg lines: 313.1 and 366.6 nm). [b] Apparent reaction rate constants for MMA (or DPB) consumption under continuous irradiation (HPK 125).

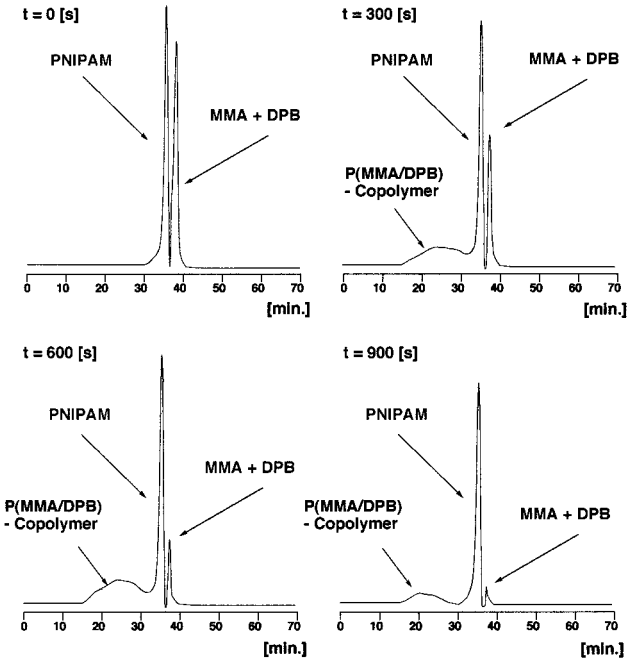

Figure 5. GPC chromatograms of the starting materials and the products formed during polymerization employing MMA/DPB and BME as photoinitiator in the reaction system PNIPAM/H_2O/DMF under continuous irradiation between 300 and 400 nm.

Table 3. (Macro)molecular Weights ($\bar{M}_n$ and $\bar{M}_w$) and Polydispersities (P_d) of the P(MMA/DPB) Polymers Formed by Photoinitiated Polymerization in the System PNIPAM/H_2O/DMF Using Benzoin (BN), Benzoin Methyl Ether (BME), and Irgacure (IGC) as Initiators

initiator		$\bar{M}_n$	$\bar{M}_w$	P_d
BN	crude	125 400	255 800	2.04
	recrystallized	130 800	247 500	1.89
BME	crude	170 500	245 000	1.44
	recrystallized	179 800	205 000	1.14
IGC	crude	105 750	251 800	2.38
	recrystallized	75 100	237 400	3.16

($\langle\Phi\rangle = 0.26 \pm 0.06$) is close to the value reported in the literature ($\Phi = 0.24$, irradiation at 313 nm in benzene[13,16]). However, the initial quantum yield of BN disappearance was significantly smaller than expected. On the other hand, the photochemical reaction of irgacure proceeded by a factor of ≈2.5 slower than anticipated. An apparent quantum yield for the photocleavage of irgacure close to unity was expected for a homogeneous reaction system.[15] These observed deviations can be explained by the existence of a microheterogeneous reaction system.[27] The distribution of the initiators between H_2O/DMF and the PNIPAM nanodomains as well as the intense scattering challenges any simple and straightforward interpretation.

Formation of P(MMA/DPB) Latex Particles in PNIPAM/H_2O/DMF. The process of P(MMA/DPB) polymerization using precipitated PNIPAM as reaction template consists of the formation of uncharged latex particles, because neither charged photoinitiators nor charged reaction templates (such as micelles or microemulsions) were used. Table 2 summarizes the apparent reaction rate constants[28] as well as the apparent initial quantum yields[28] for the consumption of MMA and DPB. Note that apparent first-order kinetics were observed. This indicates that transport processes are rate determining and that the photoinitiated polymerization process does not proceed efficiently in the H_2O/DMF bulk solution.[32] The observed kinetics demonstrate that our microheterogeneous PNIPAM template systems favors polymerization within the hydrophobic nanodomains.

GPC Analysis. The progress of the photoinitiated polymerization was monitored using GPC. A typical series of GPC chromatograms, which were performed before polymerization and at 5, 10, and 15 min, are shown in Figure 6. From these experimental results we concluded that the formation of P(MMA/DPB) polymers, possessing a distinctly bigger macromolecular weight than the template polymer (PNIPAM), is proceeding upon irradiation. Furthermore, the occurrence of a steady-state concentration of the formed P(MMA/DPB) polymers is observed. As reported previously in the Experimental Section, the created P(MMA/DPB) polymers deposit rapidly on the glass plates built in the photochemical reactor. From the quantitative analysis of the GPC peaks obtained from photolyses using BN, BME, and IGC, we estimated that 25−30% of the PNIPAM was incorporated in the formed P(MMA/DPB) precipitate.

The next step in the synthesis of P(MMA/DPB) latex particles consisted in their purification by means of reprecipitation: The polymer precipitate on the glass plates was dissolved using anhydrous THF. Then, H_2O was added until a white precipitate appeared (see Experimental Section), which was collected by filtration. The GPC chromatograms of the primary and the reprecipitated P(MMA/DPB) are shown in Figure 6. It becomes apparent that the template PNIPAM as well as the residual MMA and DPB was removed by the employed reprecipitation method. Note that only the PNIPAM, which is co-deposited beside the P(MMA/DPB)

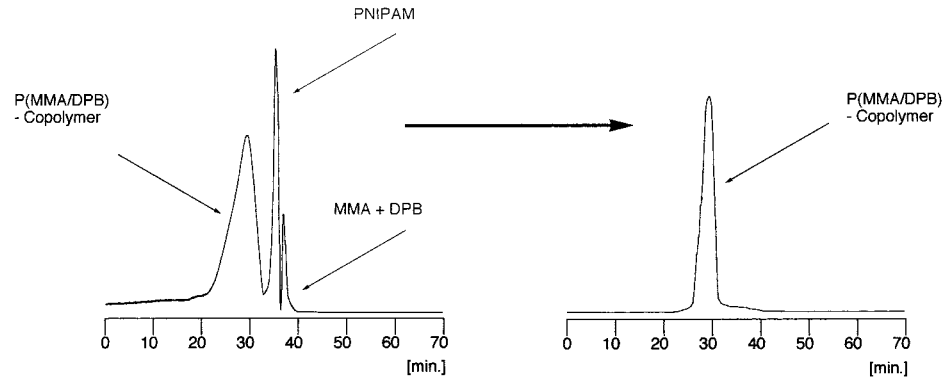

Figure 6. GPC chromatograms of the precipitate, occurring during photopolymerization of MMA/DPB/BME, on the glass scrubber plates before and after recrystallization in THF/H_2O. The recrystallization procedure is described in the text.

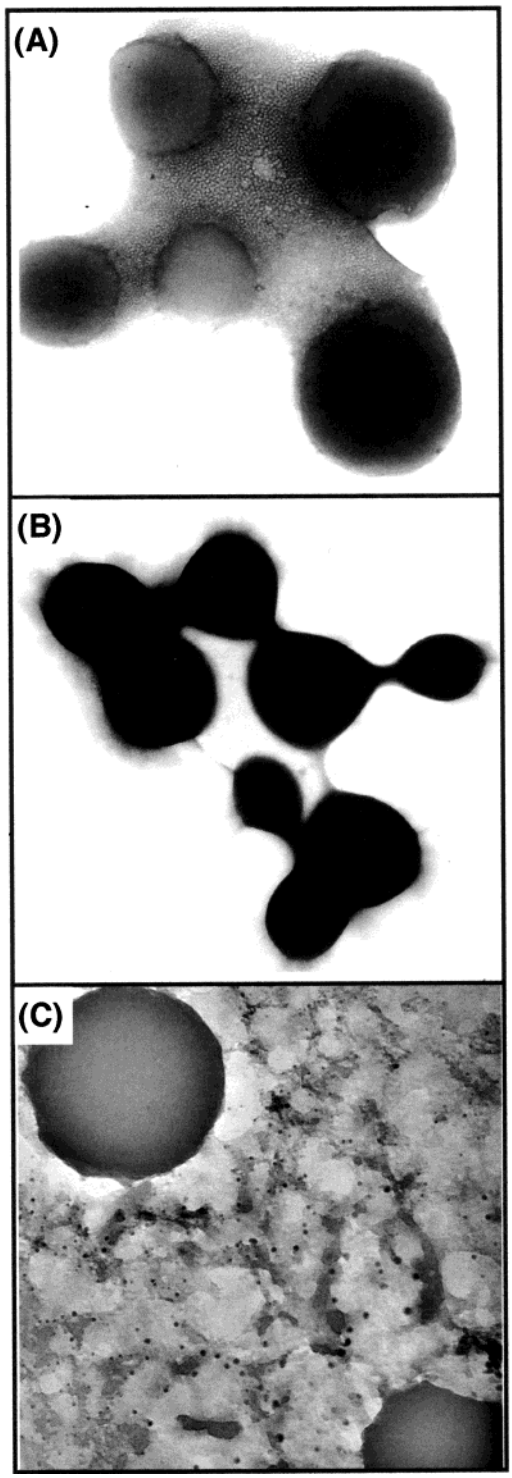

Figure 7. TEM images of the formed P(MMA/DPB) latex particles before recrystallization. The size of the images is 450 nm × 450 nm. (A) BN was used as photoinitiator. (B) BME was used as photoinitiator. (C) IGC was used as photoinitiator. Further explanations are provided in the text.

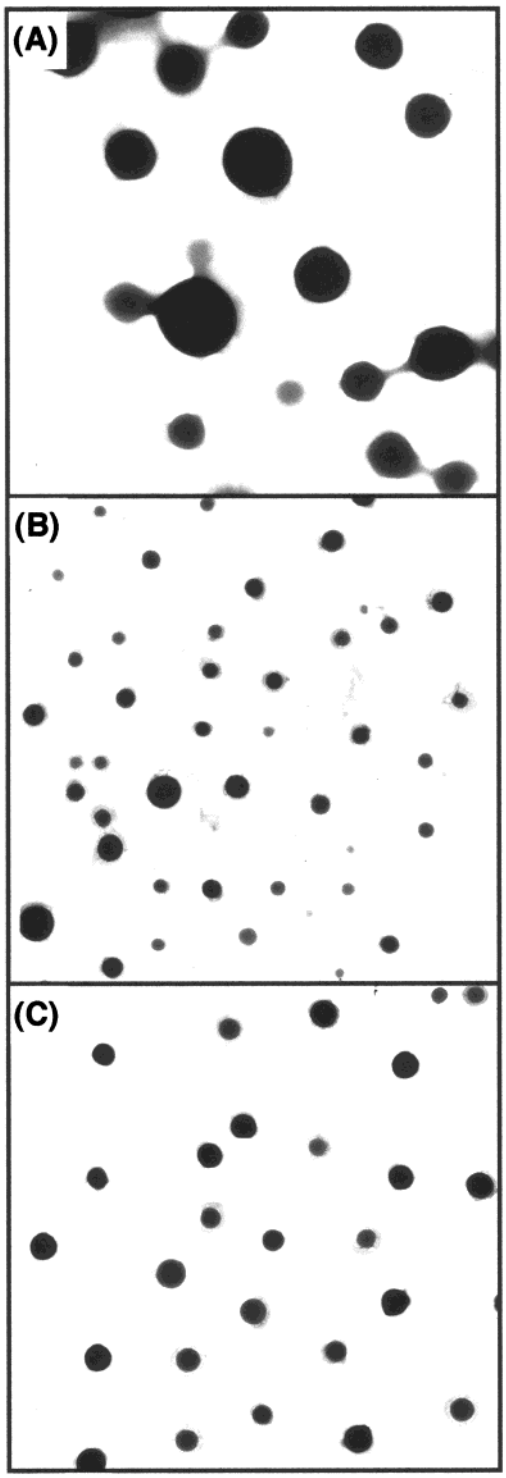

Figure 8. TEM images of the formed P(MMA/DPB) latex particles after recrystallization. The size of the images is 450 nm × 450 nm. (A) BN was used as photoinitiator. (B) BME was used as photoinitiator. (C) IGC was used as photoinitiator. Further explanations are provided in the text.

during the primary deposition at the glass plates, could be removed by this process. Any PNIPAM, which was cross-linked to P(MMA/DPB) during photopolymerization, remains within the formed latex particles.

The (macro)molecular weights[32] of the P(MMA/DPB) polymers are summarized in Table 3.

The data in Table 3 show that the macro(molecular) weights of the P(MMA/DPB) polymers exceeded the weight of the employed template macromolecule (PNIPAM, M_n = 77 400; M_w = 110 000) in all the experiments (except IGC). The process of reprecipitation led to lower average molecular weights. When BN and BME were used as photoinitiators, the polydispersity measured by GPC decreased significantly during reprecipitation. Note that the cross-linking of the P(MMA/DPB) latex particles led to duroplastic particles. On the other hand, GPC calibration was performed using monodisperse PMMA polymers. Hence, a deviation of

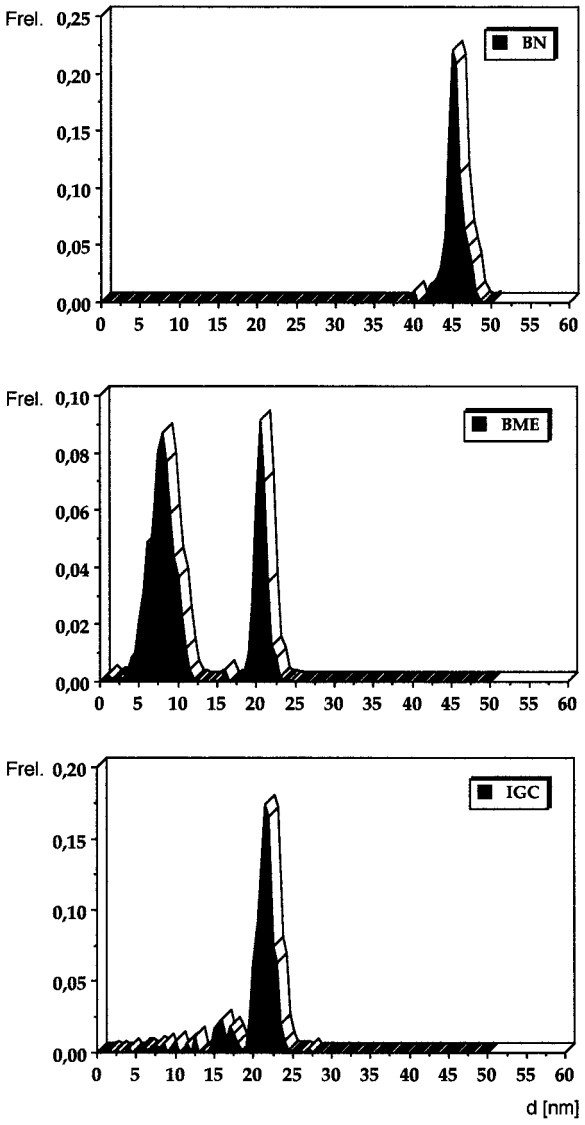

Figure 9. Size distributions of the formed P(MMA/DPB) latex particles using BN, BME, and IGC as photoinitiators after recrystallization on carbon surfaces, calculated using IMAGE.

the obtained molecular weights from the "true" values must be expected, because the physical properties of the polymers used for calibration and of the P(MMA/DPB) latex particles differ to an unknown extent. However, since the chemical composition of all P(MMA/DPB) latex particles is very similar, a relative comparison between the data obtained using BN, BME, and IGC is justified.

TEM Characterization. The characterization of the P(MMA/DPB) latex particles before and after reprecipitation revealed remarkable differences in their size distributions and their morphology. In Figure 7, typical structures obtained from the photoinitiated polymerization in the system MMA/DPB/PNIPAM/H_2O/DMF are shown. Before the process of reprecipitation, PNIPAM is clearly present in all images (e.g., as hairlike structures, latex particles such as pearls on a string, or networks interconnecting large latex particles).

In Figure 7A, BN was used as photoinitiator. Large latex particles were present (diameter: 96−145 nm), interconnected by a network of very small structures, which resemble the morphology of micelles or microemulsions.

In Figure 7B, BME was used as photoinitiator. Spherical latex particles were found (larger diameter 80−139 nm, smaller diameter 10−70 nm). Many particles were linked by linear polymer chain, which belong most likely to the PNIPAM template (pearls on a string). Furthermore, "hairy" surfaces of the latex particles can be identified.

In Figure 7C, IGC was used as photoinitiator. In this case, the largest latex particles were found (diameter: 180−220 nm). The particles possess globular shapes and are interconnected by a (PNIPAM) polymer network with embedded latex nanoparticles diameter (0.5−1.0 nm). We consider this finding as an experimental indication for the formation of latex particles by the association of very small "seeds". This mechanism was proposed earlier by Ballauf and co-workers.[6a]

The influence of reprecipitation on the morphology and size distribution of the P(MMA/DPB) latex particles becomes apparent from the comparison of Figure 7 and Figure 8, where some typical examples are presented. All the particles analyzed by TEM showed "hairy features" at the boundaries of the globular polymer particles. We attribute these amenities to the presence of PNIPAM, which becomes incorporated into the latex particles during photopolymerization. These boundary features cannot be removed by a second or a third reprecipitation. Therefore, it is likely that cross-linking between P(MMA/DPB) and PNIPAM occurs during polymer synthesis to a certain extent. The presence of PNIPAM as a hydrophobic, water-soluble polymer in the boundary region of P(MMA/DPB) latex particles enhances the water solubility of these otherwise insoluble materials. The actual PNIPAM content will be shown later in the section CHN analysis.

Computer-Assisted Analysis of the P(MMA/DPB) Morphology and Size Distribution. The analysis of all available TEM images (20−30 per experiment) was performed by the program IMAGE.[27] The size distribution of the formed (nano)structured P(MMA/DPB) latex particles is presented in Figure 9. The relative statistical maximum (F_{rel}) of the latex particle diameter was determined to $d = 46 \pm 2$ nm if BN was used as photoinitiator. A bimodal statistical distribution of particle diameters was recognized if BME was employed ($d_1 = 8.2 \pm 0.8$ nm; $d_2 = 21.0 \pm 0.5$ nm). Under those conditions, "real nanoparticles" possessing a diameter smaller than 10 nm[29] were formed (≈55 rel %) during photoinitiated synthesis. In the case of IGC serving as photoinitiator, the statistical maximum was found to be $d = 22.4 \pm 1.2$ nm.

In the ESI section, TEM images of P(MMA/PDB) latex particles formed by identical synthetic procedures in PNIPAM/H_2O/MeOH and PNIPAM/H2O/THF are shown. It becomes clear that the size distribution of the P(MMA/PDB) latex particles is determined by the nature of the cononsolvent in the microheterogeneous ternary reaction mixture. Therefore, it is very likely that the actual polymer latex (nano)particles are formed during initial photopolymerization. In addition, the extended PNIPAM network structure might isolate the growing latex (nano)particles. Thus, typical termination reactions, such as radical disproportionation[8] are suppressed.

CHN Analysis. Finally, the amount of PNIPAM incorporated into the P(MMA/DPB) latex particles during synthesis was determined using the CHN analysis method. Since PNIPAM is the only polymer employed or synthesized which contains nitrogen, its amount can be measured directly by CHN.[30] The results are summarized in Table 4. It becomes immediately clear that

Table 4. CHN Analysis of P(MMA/DPB) Synthesized Using BN, BME, and IGC as Photoinitiators before and after Reprecipitation in Comparison to the Calculated CHN Values for PNIPAM, PMMA, and PDPB[a]

polymer		C	H	N	% PNIPAM
PNIPAM	calc	63.68	9.798	12.37	100
PMMA	calc	59.98	8.054	0	
PDPB	calc	93.15	6.841	0	
P(MMA/DPB) employing	found				
BN	crude	65.71	9.745	3.578	28.9
	recrystallized	63.29	8.371	1.112	9.0
BME	crude	63.12	9.058	3.075	24.9
	recrystallized	63.03	8.001	0.512	4.1
IGC	crude	64.88	9.554	3.277	26.5
	recrystallized	63.59	8.214	0.774	6.0

[a]The PNIPAM content of the polymers was calculated according to the nitrogen content.

Scheme 2. Mechanistic Scheme of the Process of Photopolymerization Occuring in the System PNIPAM/H_2O/DMF

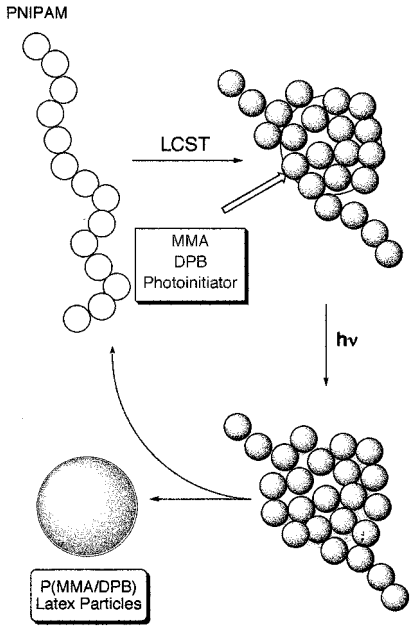

reprecipitation reduced the nitrogen content of all three P(MMA/DPB) polymer types. The PNIPAM content was calculated according to the nitrogen content of the P(MMA/DPB) polymers. The lowest PNIPAM content (4.1%) was found if BME was employed as photoinitiator. In this particular case, the P(MMA/DPB) latex particles contained 95.9% of PMMA, cross-linked by diphenylbutadiene (DPB) (ratio 10:1). The PNIPAM content was considerably higher if BN or IGC was used.

Conclusion

This work consists of a first step toward the industrial production of defined P(MMA/DPB) latex (nano)particles using PNIPAM as a template polymer in H_2O/DMF. The synthetic procedure takes advantage of the constitution of defined strongly hydrophobic nanodomains formed by collapsed PNIPAM chains in an aqueous environment. The presence of a water mixable, but hydrophobic, solvent leads to the formation of swollen PNIPAM nanodomains above its lower critical solution temperature (LCST). Those swollen nanodomains are able to absorb the strongly hydrophobic reagents MMA and DPB and the employed photoinitiators BN, BME, or IGC. Upon photoirradiation by means of a medium-pressure mercury arc lamp (HPK 125), polymerization was observed and P(MMA/DPB) polymers were formed. The isolation of growing P(MMA/DPB) (nano)particles by the PNIPAM network structure at high concentration above the LCST may support their defined formation. After the process of reprecipitation in THF/H_2O regular latex particles were found employing TEM as characterization method. The smallest diameters of the globular latex particles ($d_1 = 8.2 \pm 0.8$ nm; $d_2 = 21.0 \pm 0.5$ nm) and the lowest content of incorporated PNIPAM (4.1%) were detected using BME as photoinitiator. A schematic representation of the process investigated is given in Scheme 2.

Acknowledgment. The authors thank Prof. Dr. D. Gerthsen and Mr. M. Fotouhi Ardakani for the recording of the TEM spectra and Prof. H. Dürr for the use of his CHN facilities. The authors thank Prof. Dr. André M. Braun for the use of his facilities at the Institute of Environmental Analysis Technology (Lehrstuhl für Umweltmesstechnik) at the Engler-Bunte-Institute, University of Karlsruhe, as well as his valuable advice. Financial support from the Research Foundation of Baden-Württemberg, The German Research Foundation (DFG, BO 1060/3-1), and the Funds of the German Chemical Industry (FCI) is gratefully acknowledged.

References and Notes

(1) Segall, I.; Dimonie, V. L.; El-Aasser, M. S.; Soskey, P. R.; Mylonakis, S. G. *J. Appl. Polym. Sci.* **1995**, *58*, 385−400. Segall, I.; Dimonie, V. L.; El-Aasser, M. S.; Soskey, P. R.; Mylonakis, S. G. *J. Appl. Polym. Sci.* **1995**, *58*, 401−418. Segall, I.; Dimonie, V. L.; El-Aasser, M. S.; Soskey, P. R.; Mylonakis, S. G. *J. Appl. Polym. Sci.* **1995**, *58*, 419−426. Durant, Y. G.; Sundberg, D. C. *Macromolecules* **1996**, *29*, 8466−8472. Durant, Y. G.; Sundberg, E. J.; Sundberg, D. C. *Macromolecules* **1997**, *30*, 1028−1032.

(2) Leca, B.; Morélis, R. M.; Coulet, P. R. *Mikrochim. Acta* **1995**, *121*, 147−154.

(3) Gerharz, B.; Butt, H. J.; Momper, B. *Prog. Colloid Polym. Sci.* **1996**, *100*, 91−95. Kong, X. Z.; Kan, C. Y.; Yuan, Q. *Polym. Adv. Technol.* **1996**, *7*, 888−890. Bianco, H.; Narkis, M.; Cohen, Y. *Macromolecules* **1997**, *30*, 4978−4983. Gerharz, B.; Kuropka, R.; Petri, H.; Butt, H.-J. *Prog. Org. Coatings* **1997**, *32*, 75−80. Búcsi, A.; Forcada, J.; Gibanel, S.; Héroguez, V.; Fontanille, M.; Gnanou, Y. *Macromolecules* **1998**, *31*, 2087−2097. Duracher, D.; Sauzedde, F.; Elaissari, A.; Perrin, A.; Pichot, C. *Colloid Polym. Sci.* **1998**, *276*, 219−231. Ballauff, M. *Prog. Colloid Polym. Sci.* **1998**, *110*, 76−79. Kong, X. Z.; Ruckenstein, E. *J. Appl. Polym. Sci.* **1999**, *71*, 1455−1460.

(4) Vinogradov, G. K.; Gorwadkar, S.; Senda, K.; Morita, S. *Jpn. J. Appl. Phys.* **1994**, *33*, 6410−6414. Poulain, N.; Nakache, E.; Pina, A.; Levesque, G. *J. Polym. Sci., Part A* **1996**, *34*, 729−738. Afanasyeva, N. I.; Belogorokhov, A. I.; Blank, V. D.; Jawhari, T.; Ovchinnikov, A. A. *Macromol. Symp.* **1997**, 207−212. Liu, J.; Gan, L. M.; Chew, C. H.; Teo, W. K.; Gan, L. H. *Langmuir* **1997**, *13*, 6421−6426. Varlot, K.; Martin, J. M.; Quet, C.; Kihn, Y. *Ultramicroscopy* **1997**, *68*, 123−134. Poulain, N.; Nakache, E. *J. Polym. Sci. A* **1998**, *36*, 3035−3044.

(5) Velev, O. D.; Furusawa, K.; Nagayama, K. *Langmuir* **1996**, *12*, 2374−2384. Velev, O. D.; Furusawa, K.; Nagayama, K. *Langmuir* **1996**, *12*, 2385−2391.

(6) Weiss, A.; Dingenouts, N.; Ballauff, M.; Senff, H.; Richtering, W. *Langmuir* **1998**, *14*, 5083−5087 and references therein. Larpent, C.; Bernard, E.; Richard, J.; Vaslin, S. *Macromolecules* **1997**, *30*, 354−362.

(7) Favier, V.; Chanzy, H.; Cavaillé, J. Y. *Macromolecules* **1995**, *28*, 6365−6367. Farrell, J. R.; Iles, P. J.; Dimitrakopoulos, T. *Anal. Chim. Acta* **1996**, *334*, 133−138. Hikmet, R. A. M.; Lub, J. *Prog. Polym. Sci.* **1996**, *21*, 1165−1210. Smith, T. A.; Hotta, J.-i.; Sasaki, K.; Masuhara, H.; Itoh, Y. *J. Phys. Chem. B* **1999**, *103*, 1660−1663.

(8) Weiss, A.; Hartenstein, M.; Dingenouts, N.; Ballauff, M. *Colloid Polym. Sci.* **1998**, *276*, 794−799. Xu, J.; Li, P.; Wang,

Q.; Wu, C. *Polym. Prepr.* **1998**, *39*, 608−609. Tang, S.; Mcfarlane, C. M.; Paul, G. C.; Thomas, C. R. *Colloid Polym. Sci.* **1999**, *277*, 325−333.

(9) Zhu, P. W.; Napper, D. H. *Chem. Phys. Lett.* **1996**, *256*, 51−56.

(10) Winnik, F. M.; Ottaviani, M. F.; Bossmann, S. H.; Garcia-Garibay, M.; Turro, N. J. *Macromolecules* **1992**, *25*, 6007−6017. Winnik, F. M.; Ottaviani, M. F.; Bossmann, S. H.; Pan, W.; Garcia-Garibay, M.; Turro, N. J. *Macromolecules* **1993**, *26*, 4577−4585. Winnik, F. M.; Ottaviani, M. F.; Bossmann, S. H.; Pan, W.; Garcia-Garibay, M.; Turro, N. J. *J. Phys. Chem.* **1993**, *97*, 12998−13005 and references therein.

(11) Duracher, D.; Sauzedde, F.; Elaissari, A.; Perrin, A.; Pichot, C. *Colloid Polym. Sci.* **1998**, *276*, 219−231. Braun, D.; Schmiedel, B.; Hellmann, G. P.; Lambla, M.; Schneider, M. *Angew. Makromol. Chem.* **1998**, *254*, 79−84. Li, P.; Liu, J.; Wang, Q.; Wu, C. *Polym. Prepr.* **1998**, *39*, 606−607.

(12) Karatekin, E.; O'Shaughnessy, B.; Turro, N. J. *Macromolecules* **1998**, *31*, 7992−7995.

(13) Lewis, F. D.; Lauterbach, R. T.; Heine, H.-G.; Hartmann, W.; Rudolph, H. *J. Am. Chem. Soc.* **1975**, *97*, 1519−1525 and literature cited therein.

(14) Lipson, M.; Turro, N. J. *J. Photochem. Photobiol. A: Chem.* **1996**, *99*, 93−96.

(15) Shrestha, N. K.; Yagi, E. J.; Takatori, Y.; Kawai, A.; Kajii, Y.; Shibuya, K.; Obi, K. *J. Photochem. Photobiol. A: Chem.* **1998**, *3*, 179−186 and references therein.

(16) Hutchinson, J.; Ledwith, A. *Polymer* **1973**, *14*, 405−408.

(17) Tillmann, K.; Thust, A.; Lentzen, M.; Swiatek, P.; Förster, A.; Urban, K.; Laufs, W.; Gerthsen, D.; Remmele, T.; Rosenauer, A. *Philos. Mag. Lett.* **1996**, *74*, 309−316.

(18) Rosenauer, A.; Kaiser, S.; Reisinger, T.; Zweck, J.; Gebhardt, W.; Gerthsen, D. *Optik* **1996**, *102*, 63−69.

(19) Rosenauer, A.; Remmele, T.; Gerthsen, D.; Tillmann, K.; Förster, A. *Optik* **1997**, *105*, 99−107.

(20) Kaiser, S.; Preis, H.; Gebhardt, W.; Ambacher, O.; Angerer, H.; Stutzmann, M.; Rosenauer, A.; Gerthsen, D. *Jpn. J. Appl. Phys., Part 1* **1998**, *37*, 84−89.

(21) (a) http://www.nih.gov. (b) http://www.wuarchive.wustl.edu/packages/graphics/image-tool/.

(22) Polverari, M.; Ven, T. G. M. v. d. *Colloids Surf. A* **1994**, *86*, 209−228. Holthoff, H.; Borkovec, M.; Schurtenberger, P. *Phys. Rev. E* **1997**, *56*, 6945−6953.

(23) Winnik, F. M. *Macromolecules* **1990**, *23*, 233−242. Winnik, F. M. *Macromolecules* **1990**, *23*, 1647−1651.

(24) Odian, G. *Principles of Polymerization*; J. Wiley & Sons: New York, 1981.

(25) Bossmann, S. H.; Oliveros, E.; Göb, S.; Siegwart, S.; Dahlen, E. P.; Payawan, L., Jr.; Straub, Matthias; Wörner, M.; Braun, A. M. *J. Phys. Chem. A* **1998**, *102*, 5542−5550.

(26) Sohn, D.; Russo, P. S.; Dávila, A.; Poche, D. S.; McLaughlin, M. L. *J. Colloid Interface Sci.* **1996**, *177*, 31−44.

(27) Barrow, G. M.; Herzog, G. W. *Physikalische Chemie; Teil III: Thermodynamische und kinetische Behandlung chemischer Reaktionen*; F. Vieweg & Sohn: Braunschweig, Wiesbaden, 1983.

(28) Braun, A. M.; Maurette, M.-T.; Oliveros, E. *Photochemical Technology*; Wiley & Sons: New York, Chichester, 1991 and references therein.

(29) Pötzschke, R. T.; Staikov, G.; Lorenz, W. J.; Wiesbeck, W. *J. Electrochem. Soc.* **1999**, *146*, 141−149 and references therein.

(30) A control experiment was performed: The photoinitiated polymerization of MMA in DMF using BME as photoinitiator yielded C, 60.01; H, 8.077; N, 0.058. Therefore, it was concluded that DMF does not become incorporated into PMMA in any significant amount under our reaction conditions.

MA991608Z